Rheology and Dispersion Behavior of High-Impact Polystyrene/Ethylene–Vinyl Acetate Copolymer/TiO_2 Nanocomposites

Zhaobo Wang,[1] Guangwen Xie,[1] Xin Wang,[2] Zhikun Zhang[1]

[1]*College of Material and Environment, Qingdao University of Science and Technology, No. 53 Zhengzhou Road, Qingdao, 266042, China*
[2]*Key Laboratory of Rubber–Plastics, Ministry of Education, No. 53 Zhengzhou Road, Qingdao, 266042, China*

Received 9 February 2005; accepted 18 August 2005
DOI 10.1002/app.23713
Published online 8 March 2006 in Wiley InterScience (www.interscience.wiley.com).

ABSTRACT: TiO_2 nanoparticles were introduced into high-impact polystyrene (HIPS) in the form of a master batch in which TiO_2 was predispersed in composites of HIPS and ethylene–vinyl acetate copolymer (EVA) by melt compounding. The resulting materials were analyzed with a Rosand Precision rheometer, transmission electron microscopy, atomic force microscopy, and ultraviolet–visible light spectrophotometry. The results showed that the introduction of TiO_2 nanoparticles into HIPS influenced the apparent viscosity of the composites to a rather small extent. The addition of EVA could regulate the rheological behavior of the HIPS/TiO_2 master batch greatly. EVA helped the dispersions of the agglomerates of TiO_2 nanoparticles in the flow; this was featured by the distinct yielding in the flow after the introduction of EVA, as well as the large change in the non-Newtonian indices. The dispersions of the HIPS/TiO_2 master batch in the HIPS matrix were improved greatly by the addition of EVA. TiO_2 nanoparticles were dispersed randomly in HIPS/EVA/TiO_2 nanocomposites. The dispersion improvement of the HIPS/EVA/TiO_2 master batch was also proved by atomic force microscopy and ultraviolet–visible spectroscopy investigations. The mechanical properties of HIPS/EVA/TiO_2 nanocomposites with low TiO_2 contents were slightly higher than those of pure HIPS. J Appl Polym Sci 100: 4434–4438, 2006

Key words: dispersions; nanocomposites; polystyrene; rheology

INTRODUCTION

Polymer/inorganic nanocomposites prepared by melt compounding have become a popular topic in material science because of their markedly improved properties,[1–5] and it is well known that the monodispersed nanoparticles in a polymer matrix play an important role in the outstanding properties of nanocomposites.

Polymer/inorganic filler composites display a rather complex rheological behavior, and the influence of filler agglomerates on rheological behavior is usually shown as solidlike behaviors and yielding of the melts.[6] Also, filler particles, especially nanoparticles,[7–11] have a notable effect on the molecular mobility of polymer molecules.

The addition of antibacterial agents to a polymer is the most usual way of preventing the colonization of the polymer by microorganisms.[12] Among the numerous antibacterial agents, TiO_2 nanoparticles, typical semiconductor photocatalysts, are a kind of representative antibacterial agent.[13,14] Now TiO_2 has become one of the most promising inorganic nanoparticles in research and application fields because of its versatile function.[15,16] A lot of composites with good function are manufactured to take advantage of the special properties of TiO_2 nanoparticles.

However, the exhibition of the special properties of TiO_2 nanoparticles in the final products is determined by the dispersion condition in the polymer matrix. In contrast, in melt-compounding literature, the rheological behavior of the polymer/nanoparticle master batch is less studied, although it plays an important role in the dispersions of nanoparticles and the surface morphology of nanocomposites. In this study, high-impact polystyrene (HIPS)/ethylene–vinyl acetate copolymer (EVA)/TiO_2 nanocomposites with random dispersions of TiO_2 nanoparticles were successfully prepared via melt compounding. EVA was adopted to regulate the rheological behavior of the HIPS/TiO_2 master batch. The influence of the EVA content on the viscosity and non-Newtonian index of the HIPS/TiO_2 master batch, the dispersion morphology of the TiO_2 nanoparticles in the matrix, the mechanical properties of the nanocomposites, and the surface morphology and ultraviolet–visible (UV–vis) spectroscopy of HIPS/EVA/TiO_2 nanocomposites with low TiO_2 contents were systematically investigated.

Correspondence to: Z. Wang (wangzhb@qust.edu.cn).

EXPERIMENTAL

Materials and sample preparation

HIPS (466F type), with a melt flow index (MFI) of 4.80 g/10 min (5.0 kg at 200°C), was commercially obtained from Yangzi–BASF Co. (Nanjing, China). TiO_2 nanoparticles with an average primary particle size of 80 nm were provided by Qingdao Haier–QUST Nano Technology Research Co., Ltd. (Qingdao, China). EVA (334N type) was commercially obtained from Leuna GmbH (Leunn, Germany).

HIPS, EVA, and TiO_2 were dried for 8 h at 80, 60, and 100°C, respectively, before melt compounding. Quantitative HIPS, EVA, and TiO_2 nanoparticles were mixed under strenuous stirring, and then the mixture was granulated with a Brabender two-screw extruder (ZKS-25, Krupp Werner & Pfleiderer GmbH, Stuttgart, Germany) at 200°C with a screw speed of 80 rpm. The as-prepared HIPS/EVA/TiO_2 master batch was diluted with HIPS via melt compounding to obtain nanocomposites containing the desired TiO_2 content. The nanocomposite pellets produced by two-step melt compounding were fabricated into standard bars with an injection-molding machine (model J110EL-III Japan Steel Works, Ltd., Tokyo, Japan). The barrel temperature was set at 200°C, and the mold temperature was set at 40°C.

Characterization

The rheological behaviors of the materials were measured with Rosand Precision rheometer (Bohilin Instrument, Malvern, UK) in the double-bore experiment mode. The length/diameter ratio of the capillary in one bore was 16/1; with the orifice die in another bore was a zero-length capillary. The experiments were carried out at 200°C. The experimental results were processed with software from Bohilin Instrument, and all the rheological data obtained were subjected to Bagley and Rabinowitch calibration.

Notched specimens were tested with an API impact tester (Atlas Electric Devices Co., Chicago, IL) according to the ISO179 standard. The tests were carried out at room temperature, and the obtained data represented the average values from eight test specimens. Room-temperature tensile testing was conducted on an H10KS-0282 universal testing machine (Hounsfield Test Equipment, Redhill, UK) according to the ISO 527 standard at a crosshead speed of 10 mm/min. Five samples were tested for each case.

MFI was conducted on an MP-600 MFI instrument (Willow Grove Co., Willow Grove, PA) under the testing conditions of 200°C and 5 kg.

The dispersion morphology of TiO_2 nanoparticles in nanocomposites was observed by means of transmission electron microscopy (TEM; JEM-2000EX, JEOL, Tokyo, Japan).

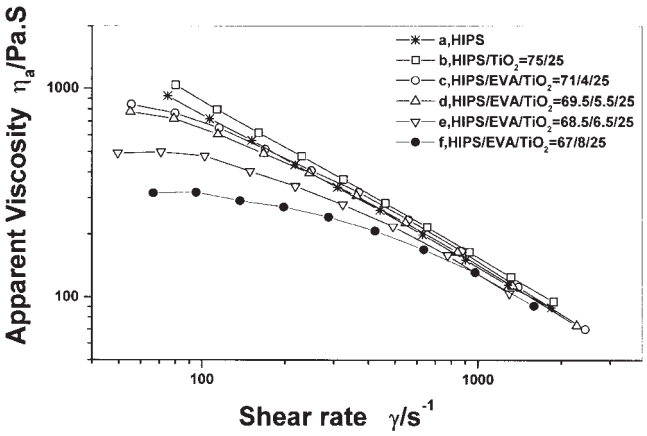

Figure 1 Flow curves of HIPS/EVA/TiO_2 master batches.

The surface scans of nanocomposite specimens were viewed by atomic force microscopy (AFM; 4410 Liestal, Nanosurf Co., Liestal, Switzerland).

The nanocomposite samples were measured in the wavelength range of 200–800 nm with a UV–vis spectrophotometer (Cary 500, Varian Co., Lake Forest, CA).

RESULT AND DISCUSSION

Rheology of the HIPS/EVA/TiO_2 nanocomposites

Figure 1 presents flow curves of the HIPS/EVA/TiO_2 master batch with different weight ratios of the raw materials. We can understand that the flow curves of pure HIPS and the HIPS/TiO_2 master batch exhibit typically pseudoplastic flow behavior; the linear regulation between the apparent viscosity and shear rate is distinct enough. Also, the apparent viscosity is influenced a bit by the addition of TiO_2 nanoparticles. To improve the flow behavior of the HIPS/TiO_2 master batch, EVA is introduced into the HIPS/TiO_2 master batch. The apparent viscosity of the composites decreases sharply with the EVA loading, and this indicates that the rheological behavior of the HIPS/TiO_2 master batch can be regulated easily by the addition of EVA. As shown in Figure 1, the curves can be easily divided into three segments in the whole shear rate according to its rheological characteristics. After the introduction of EVA, there appears the first segment, a plateau similar to Newtonian fluids at a low shear rate less than about 150 S^{-1}, at which almost no viscosity change can be found. This phenomenon indicates the relatively stable microstructure in melts of the HIPS/EVA/TiO_2 master batch, and the low shear rate lacks the ability to break it. By a comparison with the master batch with no EVA, it is evident that EVA helps the formation of the filler network because of its good wettability with TiO_2 nanoparticles. At the higher shear rate from 10^2 to 10^3 S^{-1}, the apparent

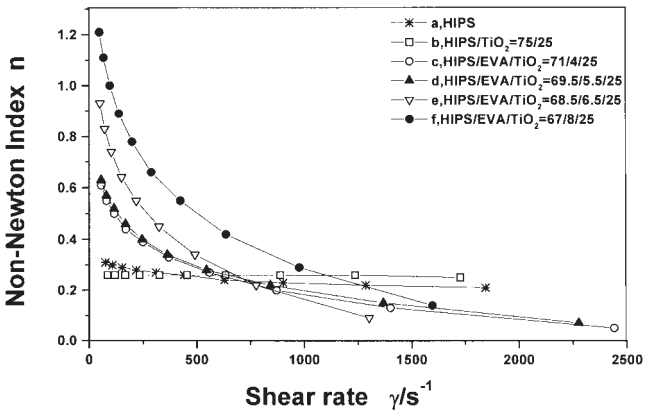

Figure 2 Dependence of non-Newtonian indices of HIPS/EVA/TiO_2 master batches on the shear rate.

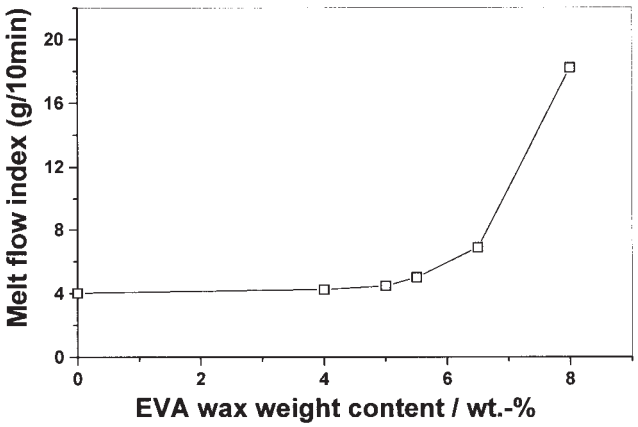

Figure 3 MFI of HIPS/EVA/TiO_2 master batches with different EVA contents (25 wt % TiO_25).

viscosity shows a smooth reduction with the shear rate, and this reveals the gradual destruction of the filler network. When the shear rate increases to more than 10^3 S^{-1}, all curves tend to overlap with one another. This indicates that the agglomerated TiO_2 nanoparticle structure has been segmented completely, and then the mobility of the HIPS molecular chains becomes the most important factor determining the apparent viscosity of the HIPS/EVA/TiO_2 master batch, so no great difference can be found among the series of master batches.

Also, the changes in the non-Newtonian indices during the flow can characterize the rheological behavior of the HIPS/EVA/TiO_2 master batch more sensitively than the apparent viscosity/shear rate curves. Therefore, it can be used to indicate the evolution of the filler network in the HIPS/EVA/TiO_2 master batch. As shown in Figure 2, the non-Newtonian index of sample b remains nearly constant, whereas the non-Newtonian index of pure HIPS decreases slightly; however, the addition of EVA to the master batch enlarges the variation range of non-Newtonian indices, and this is certainly the contribution of the filler structure evolution. Most representatively, the non-Newtonian index of the nanocomposites with high EVA contents varies from 1.2 to 0.2 with an increasing shear rate. The presence of a high non-Newtonian index greater than 1.0 provides firm evidence for the formation of a network of TiO_2 in the low shear rate region. In summary, these results elucidate clearly the solidlike flow behaviors of the HIPS/EVA/TiO_2 master batch. EVA can help the formation of the filler network at a low shear rate, which will be broken and dispersed at a high shear rate. The evolution of the filler structure can be recognized clearly from the flow curves and non-Newtonian indices.

For industrial applications, MFI is usually used to evaluate the flow capability of melts. Figure 3 shows the influence of the EVA content on the MFI of the HIPS/EVA/TiO_2 master batch. We can understand obviously that the addition of EVA improves the flow property effectively, especially when the EVA content in the HIPS/EVA/TiO_2 master batch exceeds 6 wt %; this is consistent with the analysis of Figure 1.

Dispersion morphology of the TiO_2 nanoparticles in the HIPS/EVA/TiO_2 nanocomposites

TEM was employed to prove the random dispersions of TiO_2 nanoparticles induced by the rheology improvement of the HIPS/TiO_2 master batch. Figure 4 presents a TEM picture of the TiO_2 nanoparticles in the HIPS/EVA/TiO_2 nanocomposites. The nanocom-

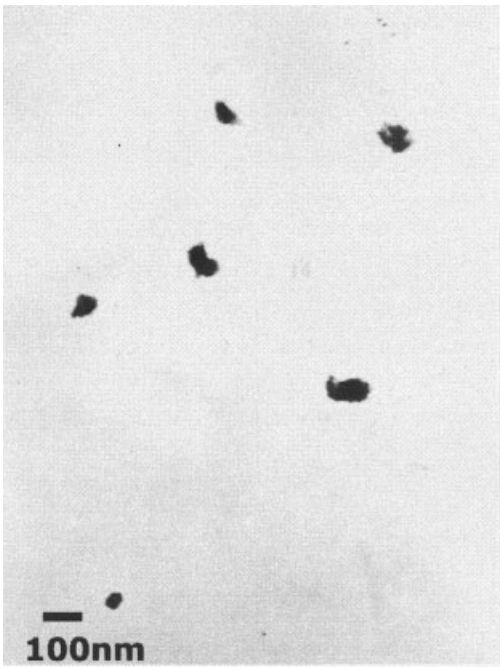

Figure 4 TEM micrograph of TiO_2 in nanocomposites (1 wt % TiO_2).

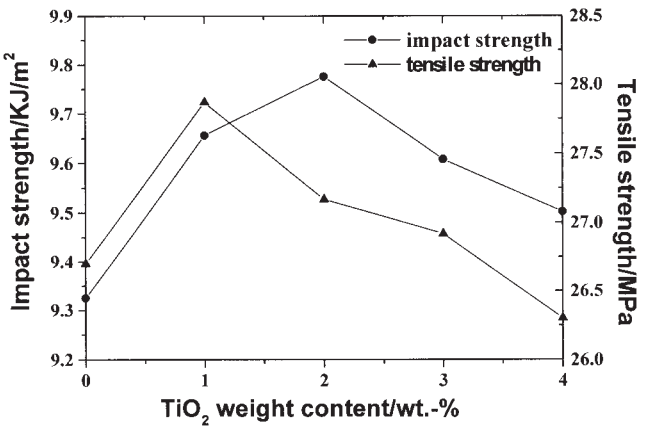

Figure 5 Influence of the TiO_2 content on the mechanical properties of HIPS/EVA/TiO_2 nanocomposites.

posites used here were prepared by the melt compounding of a blend of HIPS and sample e in Figure 4 (weight ratio = 24 : 1). The TiO_2 nanoparticles were dispersed randomly as monodispersed particles, and this was consistent with the original size.

Mechanical properties of the HIPS/EVA/TiO_2 nanocomposites

The influence of the TiO_2 content on the mechanical properties of the nanocomposites is shown in Figure 5. Nanocomposites with different TiO_2 contents were prepared by the melt compounding of a blend of quantitative HIPS and sample e in Figure 1. The notched impact strength and tensile strength increase slightly with an increase in the TiO_2 content and arrive at a maximum when the TiO_2 concentration is 2 and 1 wt %, respectively. The influence of the HIPS/EVA/TiO_2 master batch on the mechanical properties of the nanocomposites can be attributed to two factors. First, the monodispersed nanoparticles in the nanocomposites can make plastic deformation easier and lead to an increase in the mechanical properties, whereas the agglomerates of TiO_2 in the matrix become the sites of stress concentration and lead to a decrease in the impact strength. Thus, the mechanical properties of the nanocomposites are guided by the dispersion morphology of the TiO_2 nanoparticles. Second, EVA in the matrix shows a plasticization influence on the mechanical properties of the nanocomposites. In summary, the maximum of the mechanical properties is guided by the dispersion morphology of the TiO_2 nanoparticles and the plasticization of EVA synchronously. For nanocomposites with low TiO_2 contents, EVA improves the dispersion behavior of the TiO_2 nanoparticles greatly while affecting the mechanical properties of the nanocomposites only a bit.

Surface scans of the nanocomposite specimens

Figure 6 shows surface scans obtained with AFM at a low magnification. The raw materials of samples b and c in Figure 6 were a blend of HIPS and sample b in Figure 1 (weight ratio = 24 : 1) and a blend of HIPS and sample e in Figure 1 (weight ratio = 24 : 1), respectively. All specimens of Figure 6 were prepared via injection molding under the same conditions. The surface morphology of the peak and valley in Figure 6(b) is remarkable, whereas the surface of samples a and c is comparatively flat. The most striking aspect of the results is that the surface of sample c is more even compared to that of sample a. Considering the rheology difference between the HIPS/TiO_2 and HIPS/EVA/TiO_2 master batches in Figure 1, we can know that the lower viscosity of the master batch can lead to

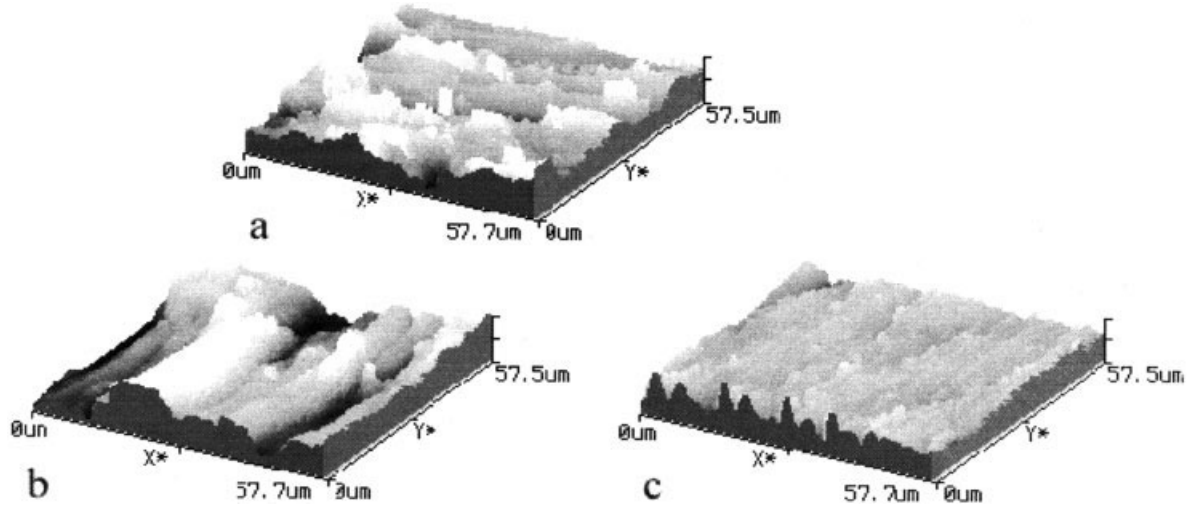

Figure 6 AFM images at 25°C of the surfaces (57.5 × 57.5 μm^2) of (a) HIPS, (b) HIPS/TiO_2 nanocomposites (1 wt % TiO_2), and (c) HIPS/EVA/TiO_2 nanocomposites (1 wt % TiO_2).

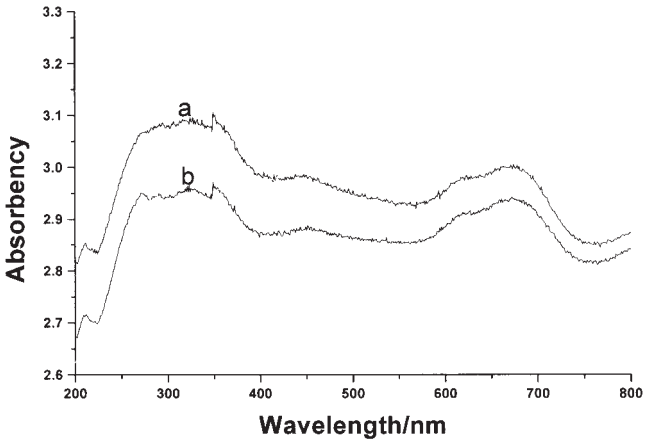

Figure 7 UV–vis spectra of the surfaces of nanocomposites (1 wt %TiO_2): (a) sample b in Figure 6 and (b) sample c in Figure 6

the good dispersions of the dispersed phase in the matrix.

UV–vis spectra of the nanocomposites are presented in Figure 7. It is evident that the absorbency of sample b is lower than that of sample a. It seems that the smooth surface of the nanocomposites reduces the light absorption in the UV-light region and in the visible range. This is consistent with the surface morphology shown in Figure 6.

CONCLUSIONS

HIPS/EVA/TiO_2 nanocomposites were prepared via melt compounding. The addition of EVA regulated the rheological behavior of the HIPS/TiO_2 master batch enormously. Besides the decrease in the apparent viscosity, EVA helped the formation of the network of the TiO_2 filler at a low shear rate, and the filler network was gradually destroyed with an increase in the shear rate. The whole evolution of the filler structure of the nanocomposites could be recognized clearly from the non-Newtonian indices of the melts. Compared with the apparent viscosity, the index could be a more sensitive parameter to reflect the structure changing in the flow.

TiO_2 nanoparticles in the HIPS/EVA/TiO_2 nanocomposites were monodispersed. The mechanical properties of the HIPS/EVA/TiO_2 nanocomposites with low TiO_2 contents were slightly higher than those of pure HIPS. The surface scans showed that the surface morphology of the nanocomposites was well improved by the addition of EVA. The dispersion improvement of the HIPS/EVA/TiO_2 master batch in the HIPS matrix was also proved by the AFM and UV–vis spectroscopy investigation.

References

1. Siochia, E. J.; Working, D. C.; Park, C. Compos B 2004, 35, 439.
2. Sandler, J. K. W.; Pegel, S.; Cadek, M. Polymer 2004, 45, 2001.
3. Ma, J.; Yu, Z. Z.; Zhang, Q. X. J Mater Chem 2004, 16, 757.
4. Wang, K. H.; Choi, M. H.; Koo, C. M. J Polym Sci Part B: Polym Phys 2002, 40, 1454.
5. Walter, P.; Mader, D.; Reichert, P.; Mulhaupt, R. J Macromol Sci 1999, 36, 1613.
6. Alexander, Y. M. Adv Polym Sci 1990, 96, 69.
7. Krishnanoorti, R.; Giannelis, E. P. Macromolecules 1997, 30, 4097.
8. Bershtein, V. A.; Egorova, L. M.; Yakushev, P. N. J Polym Sci Part B: Polym Phys 2002, 40, 1056.
9. Galgali, G.; Ramesh, C.; Ashish, L. Macromolecules 2001, 34, 852.
10. Solomon, M. J.; Almusallam, A. S.; Seefeldt, K. F. Macromolecules 2001, 34, 1864.
11. Wang, X.; Wu, Q.; Qi, Z. Polym Int 2003, 52, 1078.
12. Sauvet, G.; Dupond, S.; Kazmierski, K. J Appl Polym Sci 2000, 75, 1005.
13. Yu, J. C.; Ho, W.; Lin, J.; Yip, H.; Wong, P. K. Environ Sci Technol 2003, 37, 2296.
14. Kwak, S. Y.; Kim, S. H.; Kim, S. S. Environ Sci Technol 2001, 35, 2388.
15. Zhu, M.; Xing, Q.; He, H. Macromol Symp 2004, 210, 251.
16. Hagfeldt, A.; Graetzel, M. Chem Rev 1995, 95, 49.